NMR chemical shifts in amino acids: effects of environments, electric field, and amine group rotation

Young-Gui Yoon,* Bernd G. Pfrommer, and Steven G. Louie

Department of Physics, University of California at Berkeley, Berkeley, CA 94720, USA,

and Materials Sciences Division, Lawrence Berkeley

National Laboratory, Berkeley, CA 94720, USA.

Andrew Canning

National Energy Research Scientific Computing Center,

Lawrence Berkeley National Laboratory, Berkeley, CA 94720, USA.

(Dated: August 14, 2002)

Abstract

We present calculations of NMR chemical shifts in crystalline phases of some representative amino acids such as glycine, alanine, and alanyl-alanine. To get an insight on how different environments affect the chemical shifts, we study the transition from the crystalline phase to completely isolated molecules of glycine. In the crystalline limit, the shifts are dominated by intermolecular hydrogen-bonds. In the molecular limit, however, dipole electric field effects dominate the behavior of the chemical shifts. We show that it is necessary to average the chemical shifts in glycine over geometries. Tensor components are analyzed to get the angle dependent proton chemical shifts, which is a more refined characterization method.

I. INTRODUCTION

Nuclear magnetic resonance (NMR) chemical shifts measure the local induced magnetic field on a nucleus, which is sensitive to the chemical environments. They can be useful as fingerprints for detailing the structure and chemical composition of condensed matter systems. The NMR chemical shifts are becoming increasingly important for the characterization of biomolecules, specially for proteins[1,2], which motivated the present work on the amino acids, glycine, alanine, and a very simple peptide, alanyl-alanine. A systematic study of the NMR chemical shifts of proteins and amino acids, the building blocks of proteins, is highly desired, to lay the foundations for subsequent studies of protein shifts in complex biological environments. Some features can be revealed by investigating intermediate configurations between known crystalline phases and completely isolated molecules. Nevertheless, only recently it has become possible to calculate in an *ab initio* fashion the NMR chemical shifts of extended system[5–9].

In this study, we present first NMR chemical shift calculations of amino acids in the condensed phase. The crystalline phase of some representative amino acids such as glycine, alanine, and alanyl-alanine are investigated. We analyze proton chemical shifts in glycine systematically to address the effects of the environments, including the effect of the electric field in the molecular limit and that of amine group rotation. Finally, the angular dependence of chemical shifts for crystalline glycine from the computed chemical shift tensor is presented.

The calculation of the proton shifts in configurations between that of a crystal and an isolated molecule suggests the potential of using NMR chemical shifts for the analysis of the solvent effects and effects of environments in the real protein conformations. The proton shifts in the crystalline limit are dominated by the effects of hydrogen-bonded oxygen atoms, while the trend in the shifts in the molecular limit is attributed to long-range electric field.

It is well known that amine and methane groups can rotate at ambient temperature in crystalline phases of amino acids at a rate that is too fast to resolve the three protons in these groups with NMR chemical shift experiments[3,4]. Indeed, there is only one observed chemical shift corresponding to protons belonging to an amine or a methane group of α-glycine and L-alanine. To be consistent with experiments, the calculated chemical shifts also have to be averaged accordingly. First, we performed a single NMR calculation with the equilibrium geometries, and the chemical shifts are averaged over the three equivalent protons belonging

to an amine or a methane group of the α-glycine and L-alanine. The procedure considers three different sites of protons per each rotating group. Second, we explicitly rotated the amine group of the α-glycine by the finite angles of ± 30, and 60 degrees around the axis connecting the proton center of mass and the nitrogen of the amine group, and performed three additional NMR calculation with those geometries. Then, the glycine chemical shifts are averaged over the equilibrium and three additional geometries, which leads to a total of twelve different proton site considered per per the rotating amine group of the α-glycine. This averaging procedure improves the agreement with experiment substantially.

NMR chemical shift tensors are more refined in characterizing biomolecules than just the isotropic shifts. We therefore perform calculation of the chemical shift anisotropies of proton in solids here for the first time. As an example of the use of NMR chemical shifts tensors, we present the theoretical angular dependence of chemical shifts from an anisotropy tensor for crystalline glycine, and compare the results with experiments. We obtain reasonable qualitative agreement with experiments, and demonstrate that theory can be used to refine and interpret experimental data.

II. STRUCTURE

We present NMR chemical shifts of crystalline phases of α-glycine, L-alanine, and L-alanyl-alanin. The crystal α-glycine (NH_2CH_2COOH)[10] with space group $P2_1/n$ and L-alanine (NH_2CHCH_3COOH)[11] with space group $P2_12_12_1$ are selected because of their simple geometry. L-alanyl-L-alanine $(H(NHCHCH_3CO)_2OH)$[12] with space group I4 is included as a dipeptide prototype. Since highly reliable neutron scattering data are available for the structure of α-glycine[10] and L-alanine[11] for the heavier elements, we relax only the position of the hydrogen atoms within the local density approximation to get an accurate geometry. For L-alanyl-L-alanine, no neutron diffraction data are available to our knowledge. Therefore, we relax the whole structure starting from the geometry as given by the X-ray diffraction experiments[12].

III. PLANEWAVE AND PSEUDOPOTENTIAL PARAMETERS

In NMR measurements, the chemical shift is one third of the trace of the chemical shift tensor, $\sigma(\mathbf{r}) = \text{Tr}[\overset{\leftrightarrow}{\sigma}(\mathbf{r})]/3$, which connects the induced magnetic field to the external uniform applied magnetic field, $\mathbf{B}_{\text{in}}(\mathbf{r}) = -\overset{\leftrightarrow}{\sigma}(\mathbf{r})\mathbf{B}_{\text{ext}}$. We compute σ following Ref. [6] and Ref. [8]. The electronic structure is described using density functional theory in the local density approximation with pseudopotentials. We expand the wave functions in a plane wave basis set up to an energy cut-off of 100 Ry. Test of our pseudopotentials for C and N have been reported previously[6,8].

Following the experimental convention, we will quote chemical shifts with respect to standard reference systems of a neat liquid sample with spherical shape at 300K. The C,H shifts are given with respect to tetramethylsilane (TMS) by $\delta_{\text{TMS}}(\text{sample}) = -[\sigma(\text{sample}) - \sigma(\text{TMS})]$, where σ is the absolute chemical shift. For N, nitromethane is used as standard: $\delta_{\text{CH}_3\text{NO}_2}(\text{sample}) = -[\sigma(\text{sample}) - \sigma(\text{CH}_3\text{NO}_2)]$. We do not directly compute $\sigma(\text{TMS})$ and $\sigma(\text{CH}_3\text{NO}_2)$; for the H δ_{TMS}, we fix $\sigma(\text{TMS})$ by imposing that the computed value of δ_{TMS} for gas CH_4 is equal to the experimental value of 0.13 ppm[13]. For the C δ_{TMS} and the N $\delta_{\text{CH}_3\text{NO}_2}$, we use the procedure in Ref. [8].

IV. RESULTS AND DISCUSSION

Tables I and II show the computed H, C, and N chemical shifts for the amino acids studied in their crystalline phase. Overall agreement with experiment is good. For the carbon chemical shifts, the calculated shifts are compared with four available experimental data sets[19,21,23,24]. All four experiments employed the cross-polarization technique, and two of them[19,23] also employed the magic-angle spinning technique. The α-glycine carbon shift is compared with two different experiments, and two sets of experimental data are essentially the same. The agreement with the experiments is dependent on the kind of carbons. The dependence repeats in the case of the L-alanine and L-alanyl-L-alanie carbon chemical shifts as well. To analyze the dependence, notice that there are two kinds of hybridization for carbon atoms. First, C(2) of α-glycine, C_α, C_β of L-alanine, and C(1), C(2), C(4), C(5) of L-alanyl-L-alanine has sp^3 hybridization. Second, C(1) of α-glycine, C of L-alanine, and C(3), C(6) of L-alanyl-L-alanine has sp^2 hybridization. The sp^2 hybridized

4

carbons tend to agree less well with experiment than the sp^3 hybridized ones, consistent with previous calculations[6,8]. This discrepancy is not too important because carboxylic or peptidic carbons are irrelevant in assigning the kinds of peptides[14]. The nitrogen chemical shifts agree well with available experimental data. The α-glycine nitrogen shift is compared with the magic-angle spinning cross-polarization experiment[19], and the L-alanyl-L-alanine nitrogen shifts is compared with cross-polarization experiment[24]. Excellent agreement with proton chemical shift experiments in the literature is obtained. For α-glycine experiments, ^{1}H CRAMPS (combined rotation and multiple pulse spectroscopy)[19] and solid-state multiple pulse spectroscopy for deuteron NMR[18] methods were used in the references. Our theoretical calculations agree better with more recent and more accurate ^{1}H CRAMPS results. However, no tensor data were reported for the ^{1}H CRAMPS experiment, and only the deuteron data were used for the comparison of calculated tensor data. For L-alanine proton chemical shifts, very recent experimental data by solid-state ultrafast magic-angle spinning ($\omega_R/2\pi = 35$kHz)[22] are compared.

Focusing on the proton chemical shifts of amine group in glycine, the shifts that are not averaged somewhat deviate from experiment. Theoretical proton chemical shifts in the same amine group differ from each other by as much as 5.8 ppm, although there is only one observed peak in experiment corresponding to these hydrogen atoms. This is not unexpected because the amine and methane group of amino acids in the crystalline phase are known to rotate over a wide range of temperature[3,4]. The experimental rate of amine group rotation from the spin-lattice relaxation (T_1) measurement and Arrhenius expression of correlation time is found to be around 10^9 per second[4]. This dynamical motion cannot be resolved in typical NMR chemical shifts measurements, and the motion averages the shifts over the rotation. To investigate the dynamical effect, we compare chemical shifts calculated with the single relaxed equilibrium geometry of the glycine to those averaged over the geometries corresponding to amine group rotations in Table I. The chemical shifts calculated with the single geometry are shown in parentheses in Table I. In the other case, we average the proton shifts of glycine in the crystalline phase over geometries obtained by rotating the amine group by 0, $\pm$30, and 60 degrees around the axis connecting the proton center of mass and the nitrogen of the amine group using the structures in Fig. 1 as reference. We average over protons in the same amine group, since they are not resolved in the time scale of NMR experiments. The agreement with experiment is now significantly improved. The

averaged proton chemical shifts with rotation reduce the error by half. This calculation also shows that the effects of rotation of amine group can be reasonably well described with relatively small sampling of motion. We note that amine group rotation does not affect the atoms that do not belong to amine group. Only the nitrogen shift is affected appreciably.

For a better understanding of the proton chemical shifts, we analyze the tensor components of the proton chemical shifts in glycine (Fig. 3, 4, and 5). Chemical shift tensors can be obtained by measuring the angle dependence of the shifts. In such a measurement, an external magnetic field is applied in a direction perpendicular to the axis of rotation of a crystal, and the chemical shift spectra are measured as a function of rotation angle. The rotation axes are perpendicular to the applied external field, and the axes are defined as in the reference[18]. The a*-axis is the crystal a-axis and b*-axis is the crystal b-axis, and they are orthogonal. c*-axis is chosen to be the axis perpendicular both to a*-axis and b*-axis, and is not the same as crystal c-axis. Azimuthal angles of Fig. 3 are obtained by mapping the a*-axis, b*-axis, and c*-axis to the z-axis, x-axis, and y-axis respectively and taking the azimuthal angles of the external magnetic fields in the xy-plane. Similarly, azimuthal angles of Fig. 4 and Fig. 5 are obtained by taking the cyclic permutation of the x-axis, y-axis, and z-axis in the mapping. The important features are summarized in Table III, and the eigenvalues and eigenvectors of the tensor data are summarized in Table IV. There are four glycine molecules in the unit cell, and there are inequivalent sets of molecules whenever we apply the external magnetic field which is not perpendicular to the unique b-axis. We prepared our coordinates from the neutron diffraction data[10], the proton coordinates shown in the reference and the coordinates obtained from inversion symmetry define the first set. All other coordinates defines the second set, and the numbers in the parentheses in Table III and IV represent the second set whenever they differ from those of the first set. Similarly, the thick lines of Fig. 3, and 5 represent the first set, and the thin lines of them represent the second set. In Fig. 4, both the data sets have the same values. In Table III, experiments are performed on deuterons, and the experimental chemical shift data shown in the table are read from the plot in the reference[18]. The experimental angles of maxima and minima of chemical shifts of each plot, however, are obtained from the fitting curve provided in the reference because of the scattered raw data profile. Since the experimental data have no explicit reference material, to make meaningful comparison with our theoretical calculation, we subtracted isotropic part of the chemical shifts calculated from the average of six minima

and maxima of the data read and shown in the table. The agreement of the overall shape and phase of theoretically calculated angle dependent chemical shifts with those of experiments[18] is reasonably good. The isotropic parts of chemical shifts are slightly overestimated (Table I), and some of the difference between σ_{max} and σ_{min} deviates from experiments. In Table IV, anisotropy data obtained from experimental fit are compared with theoretical calculations. Considering that the unfitted experimental data points are also scattered, the quality of the eigenvectors and eigenvalues form the curve fit may not be as good as the original unfitted data, and our theoretical calculations can be used to refine and interpret the experiments. The angular dependence of chemical shifts tells the details of the anisotropy of the shifts, and therefore, more likely to be affected by the atoms in the surroundings. The overall angle dependence of H(5) is smaller than H(4) both in theory and in experiments. The trend can be because H(5) has no hydrogen-bonded oxygen neighbor, whereas H(4) has two.

We study the effects of environments on the chemical shifts in glycine by calculating configurations between the known crystalline phase and completely isolated molecules, keeping the geometry of individual molecules to be that in the crystal but with increasing intermolecular distances (Fig. 6). Chemical shifts at infinite volume per molecule is extrapolated from a separate set of supercell calculations to get values that are accurate and independent of our choice of intermediate configurations. The proton chemical shifts as a function of the inverse volume per molecule are fairly linear if the intermolecular neighbor distance in the crystal is around 4 Åor larger. Since the electric field of a dipole moment is proportional to the inverse of the volume per molecule in the molecular limit, the linearity at large distance indicates the influence of long-range electric field effects of the neighboring molecules. The proton chemical shifts in this study may shed a light on the trend of the proton chemical shifts in proteins. Unlike ^{19}F chemical shifts in proteins, which are expected to have a 10 ppm range from electrostatic interaction[1], the proton chemical shifts in proteins is estimated to be less sensitive to electric field with a range less than 1 ppm. The significant feature of proton chemical shifts in protein folding will be hydrogen-bonding, which is also pointed out in the reference[1]. Most of the change in the proton chemical shifts between the two limits in Fig. 6 is attributed to nearest intermolecular neighbor oxygen atoms. H(1), H(3), and H(4) have two adjacent oxygen atoms that do not belong to the single glycine molecule unit. H(2) has only one such oxygen atom, and H(5) has no such oxygen atom. To see the relation between the oxygen-hydrogen distance d_{OH} and the chemical shift, we tabulated

the quantity obtained by multiplying d_{OH}^3 and the difference of the H(2) chemical shift from that the isolated configuration in Table V. We didn't tabulated the product in which d_{OH} exceeds 4 Åbecause, then, the second nearest d_{OH} is comparable to the nearest d_{OH}. Robust linearity is found between the chemical shifts and the inverse of the third power of the intermolecular distance in the hydrogen H(2) which has only one intermolecular neighbor oxygen. This is not new in the literature. The same relation between proton chemical shifts with hydrogen bond length in water dimer was reported before[20]. In Fig. 7, we present residual chemical shifts after subtracting the nearest intermolecular neighbor oxygen contribution by assuming a $\delta\sigma[O_{nearest}] = 138.54$ ppm au^3/d_{OH}^3 relation following Ref [20]. Indeed, 138.54 ppm au^3 is quite close to the quantities tabulated in Table V, and the discrepancy can be attributed to the fact that there are other distant oxygen atoms in the surroundings and that the model does not necessarily take the all possible details of quantum mechanical effects. However, the major contribution of the chemical shift change in the small intermolecular oxygen-hydrogen distance limit is well described by the empirical formula. Since the scale of chemical shift change in the case that a proton approaches oxygen atoms is very large compared to the scale of the change when the proton is far away from the oxygen atoms, the distribution of the proton chemical shifts is expected to carry information on the existence of oxygen atoms in unknown environments. Therefore, proton chemical shifts might be a good oxygen probe insensitive to a long-range electric field.

V. CONCLUSION

In summary, our calculations demonstrate that NMR chemical shift calculation can be helpful in understanding effects of environments in amino acids and the dynamical effects of rotating amine groups. Effects of environments on glycine proton chemical shifts in the crystalline limit is dominated by the intermolecular hydrogen-bond with oxygen atoms like in water, and those in the molecular limit are attributed to long-range electric field of dipole moments of neighboring molecules. Proton chemical shifts averaged over amine group rotations are expected to mimic the correct number of peaks and their positions in experiments.

Acknowledgments

* Current address: Princeton Materials Institute, Princeton University, Princeton, NJ 08544, USA.

[1] A. de Dios, J. G. Pearson, and E. Oldfield, Science **260**, 1491 (1993).

[2] A. de Dios, J. Pearson, and E. Oldfield, J. Am. Chem. Soc. **115**, 9768 (1993).

[3] G. R. Kneller, W. Doster, M. Settles, S. Cusack, and J. C. Smith, J. Chem. Phys. **97**, 8864 (1992).

[4] Z. Gu, K. Ebisawa, and A. McDermott, Sol. Stat. Nuc. Mag. Res. **7**, 161 (1996).

[5] F. Mauri, B. G. Pfrommer, and S. G. Louie, Phys. Rev. Lett. **77**, 5300 (1996).

[6] F. Mauri, B. G. Pfrommer, and S. G. Louie, Phys. Rev. Lett. **79**, 2340 (1997).

[7] F. Mauri, A. Pasquarello, B. G. Pfrommer, Y.-G. Yoon, and S. G. Louie, Phys. Rev. B **62**, R4786 (2000).

[8] Y.-G. Yoon, B. G. Pfrommer, F. Mauri, and S. G. Louie, Phys. Rev. Lett. **80**, 3388 (1998).

[9] B. G. Pfrommer, F. Mauri, and S. G. Louie, J. Am. Chem. Soc. **122**, 123 (2000).

[10] P. Jönsson and Å. Kvic, Acta Cryst. B **28**, 1827 (1972).

[11] M. Lehmann, T. Koetzle. and W. Hamilton, J. Am. Chem. Soc. **94**, 2657 (1972).

[12] R. Fletterick, C. Tsai, and R. Hughes, J. Phys. Chem. **75**, 918 (1971).

[13] W. Kutzelnigg, U. Fleischer, and M. Schindler, in *NMR basic principles and progress*, P. Diehl (eds.) (Springer-Verlag, New York, 1990), No. 23.

[14] T. E. Creighton, *Proteins Structures and Molecular Properties*, (W. H. Freeman and Company, New York, 1993).

[15] For C, to convert $\delta_{benzene}$ of experimental data to δ_{TMS} we use $\delta_{TMS}(C, benzene) = 128.5$ ppm[13].

For N, to convert $\delta_{\mathrm{NH_3(liquid)}}$, and $\delta_{\mathrm{NH_4Cl(sqturated)}}$ of experimental data to $\delta_{\mathrm{CH_3NO_2(liquid)}}$ we use $\delta_{\mathrm{CH_3NO_2(liquid)}}(\mathrm{N, NH_3(liquid)}) = $ -380 ppm[16] and $\delta_{\mathrm{CH_3NO_2(liquid)}}(\mathrm{NH_4Cl(sqturated)}) = $ -359.5 ppm[17].

[16] C. J. Jameson, A. K. Jameson, D. Oppusunggu, S. Wille, P. M. Burrell, and J Mason, J. Chem. Phys. **74**, 81 (1981).

[17] G. Martin, M. Martin, and J. Gouesnard, in *NMR basic principles and progress*, P. Diehl (eds.) (Springer-Verlag, New York, 1981), No. 18.

[18] C. Müller, W. Schajor, H. Zimmermann, and U. Haeberlen, J. Mag. Res. **56**, 235 (1984).

[19] H. Kimura, K. Nakamura, A. Eguchi, H. Sugisawa, K. Deguchi, K. Ebisawa, E.-I. Suzuki, A. Shoji, J. Mol. Str. **447**, 247 (1998).

[20] R. Ditchfield, J. Chem. Phys. **65**, 3123 (1976).

[21] R. A. Haberkorn, R. E. Stark, H. van Willigen, and R. G. Griffin, J. Am. Chem. Soc. **103**, 2534 (1981).

[22] I. Schnell, A. Lupulescu, S. Hafner, D. E. Demco, and H. W. Spiess, J. Mag. Res. **133**, 61 (1998).

[23] A. Naito, S. Ganapathy, K. Akasaka, and C. A. McDowell, J. Chem. Phys. **74**, 3190 (1981).

[24] C. Hartzell, M. Whitfield, T. G. Oas, and G. P. Drobny, J. Am. Chem. Soc. **109**, 5966 (1987).

Atoms	δ_{ref}	
	theory [ppm]	experiment [ppm]
H(1)	(12.8)	
H(2)	(10.1)	
H(3)	(7.0)	
H(1),H(2),H(3) averaged	9.0(10.0)	7.8 [18], 8.5 [19]
H(4)	6.2(6.0)	4.3 [18], 4.4 [19]
H(5)	4.0(3.9)	3.5 [18], 3.4 [19]
C(1)	151(153)	177 [21], 176 [19]
C(2)(C$_\alpha$)	44(44)	46 [21], 44[19]
N	-321(-334)	-348 [19]

TABLE I: Computed NMR chemical shifts (δ_{ref}) for crystalline α-glycine. The δ_{ref} means Hδ_{TMS}, Cδ_{TMS}, or N$\delta_{\mathrm{CH_3NO_2}}$. The second column labels each atom. Reference materials are liquid TMS for C, and H, and liquid CH_3NO_2 for N^{15}. See text for the explanation of numbers in parentheses. The atom labels are from Ref. [10].

	Atoms	δ_{ref}	
		theory	experiment
		[ppm]	[ppm]
L-alanine	H^{α}	4.9	3.6 [22]
	H^1,H^2,H^3 averaged	10.7	8.4 [22]
	$H^{\beta 1},H^{\beta 2},H^{\beta 3}$ averaged	2.2	1.2 [22]
	C	154	177 [23]
	C_{α}	51	51 [23]
	C_{β}	22	20 [23]
	N	-320	
L-alanyl-	C(1)	20	
L-alanine	C(2)	47	
	C(3)	150	170 [24]
	C(4)	50	
	C(5)	20	
	C(6)	156	
	N(1)	-327	
	N(2)	-257	-260 [24]

TABLE II: Computed NMR chemical shifts (δ_{ref}) for L-alanine and L-alanyl-L-alanine. The δ_{ref} means Hδ_{TMS}, Cδ_{TMS}, or N$\delta_{\mathrm{CH_3NO_2}}$. The second column labels each atom. Reference materials are liquid TMS for C, and H, and liquid CH_3NO_2 for N^{15}. The atom labels are from Ref. [11] for L-alanine and Ref. [12] for L-alanyl-L-alanine. In Ref. [22], data are read from the ultrafast MAS plot.

	a*-axis rotation		b*-axis rotation		c*-axis rotation	
	theory	experiment	theory	experiment	theory	experiment
H(1,2,3)						
$\sigma_{max} - \sigma_{min}$	4.5	4.8	3.5	4.4	1.6	3.8
$\frac{\sigma_{max} + \sigma_{min}}{2} - \sigma_{iso}$	0.4	0.3	0.9	1.2	-1.3	-1.4
φ of σ_{max}	96 (84)	105	8	20	26 (154)	50
φ of σ_{min}	6 (174)	15	98	110	116 (64)	140
H(4)						
$\sigma_{max} - \sigma_{min}$	16.8	9.2	3.8	2.8	16.0	10.4
$\frac{\sigma_{max} + \sigma_{min}}{2} - \sigma_{iso}$	2.8	1.1	-4.7	-3.0	1.9	1.9
φ of σ_{max}	163 (17)	165	148	112	100 (80)	107
φ of σ_{min}	73 (107)	75	58	22	10 (110)	17
H(5)						
$\sigma_{max} - \sigma_{min}$	4.3	1.6	4.0	4.8	4.5	4.6
$\frac{\sigma_{max} + \sigma_{min}}{2} - \sigma_{iso}$	-1.1	-2.6	1.2	0.8	-0.2	0.2
φ of σ_{max}	65 (115)	115	58	74	3 (177)	10
φ of σ_{min}	155 (25)	25	148	164	93 (87)	100

TABLE III: Comparison of experimental measurement and theoretical calculation of angular dependence of chemical shifts. See text for the explanation of numbers in parentheses. The unit of all chemical shifts is ppm, and the unit of all angles is degree.

Site	Eigenvalues [ppm]			Polar angles of eigenvector					
		theory	experiment		$\vartheta[°]$ theory	experiment		$\varphi[°]$ theory	experiment
H(1,2,3)	$\sigma_{xx} =$	-6.58	-2.66	$\mathbf{e}_x$	85.5	83.1		91.5 (268.5)	130.8
	$\sigma_{yy} =$	-4.44	-0.09	$\mathbf{e}_y$	65.9	86.0		359.5 (0.5)	40.3
	$\sigma_{zz} =$	-11.02	2.75	$\mathbf{e}_z$	24.5	8.0		191.4 (168.6)	281.4
	$\Delta\sigma$(theory) $= 16.5$ ppm, η(theory) $= 0.194$								
	$\Delta\sigma$(experiment) $= 4.1$ ppm, η(experiment) $= 0.993$								
H(4)	$\sigma_{xx} =$	-7.83	-4.55	$\mathbf{e}_x$	60.3	19.2		21.2 (338.8)	44.1
	$\sigma_{yy} =$	-3.09	-1.71	$\mathbf{e}_y$	46.8	105.8		171.6 (188.4)	6.6
	$\sigma_{zz} =$	10.92	6.26	$\mathbf{e}_z$	78.1	100.7		276.6 (83.4)	99.7
	$\Delta\sigma$(theory) $= 16.4$ ppm, η(theory) $= 0.434$								
	$\Delta\sigma$(experiment) $= 9.4$ ppm, η(experiment) $= 0.454$								
H(5)	$\sigma_{xx} =$	-3.11	-2.25	$\mathbf{e}_x$	72.3	117.9		262.6 (97.4)	77.6
	$\sigma_{yy} =$	-0.15	-0.87	$\mathbf{e}_y$	47.0	42.0		124.3 (235.7)	131.6
	$\sigma_{zz} =$	3.27	3.12	$\mathbf{e}_z$	52.8	61.5		25.6 (334.4)	4.4
	$\Delta\sigma$(theory) $= 4.9$ ppm, η(theory) $= 0.905$								
	$\Delta\sigma$(experiment) $= 4.7$ ppm, η(experiment) $= 0.438$								

TABLE IV: Comparison of chemical shift tensors in α-glycine. The experimental chemical shift data shown in the table are from the table 2 in the reference[18]. Isotropic part of the chemical shifts are compared in Table I. Polar angles are defined in the standard orthogonal frame with mapping the a*-axis, b*-axis, and c*-axis to the z-axis, x-axis, and y-axis respectively[18]. See text for the explanation of numbers in parentheses.

O-H distance d_{OH} [au]	$H\delta_{TMS}$ [ppm]	$(H\delta_{TMS}(d_{OH}) - H\delta_{TMS}(\infty))d_{OH}^3$ [ppm au^3]
3.398	10.08	157
3.732	9.03	154
4.163	8.11	147
4.731	7.41	141
5.508	6.92	141
6.638	6.61	156
∞	6.07	—

TABLE V: Relation between oxygen-hydrogen distance d_{OH} and the chemical shifts of H(2) in α-glycine.
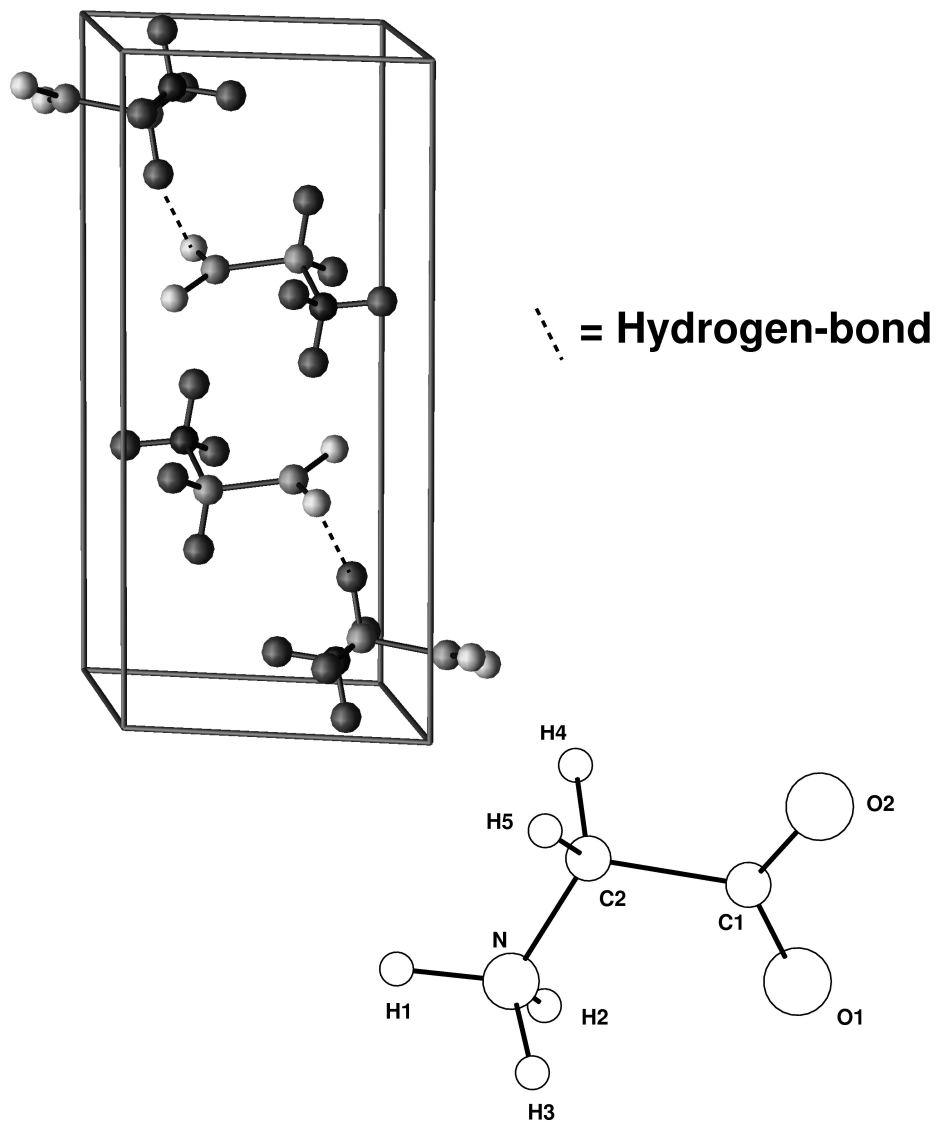
FIG. 1: Hydrogen bonds in crystalline glycine ($C_2H_5NO_2$) and a ball-and-stick model of a glycine monomer in the crystalline geometry.

Alanine
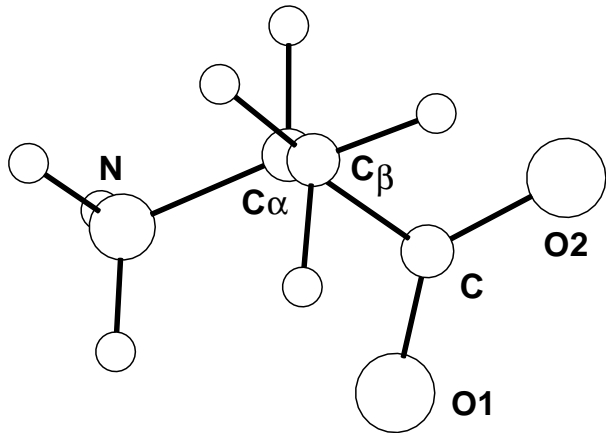
Alanyl–alanine
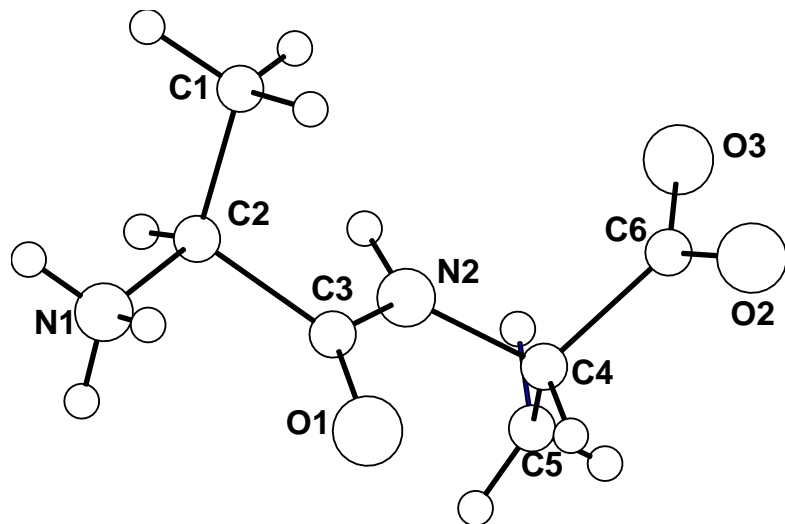
FIG. 2: Ball-and-stick model of alanine ($C_3H_7NO_2$) and alanyl-alanine ($C_6H_{12}N_2O_3$).
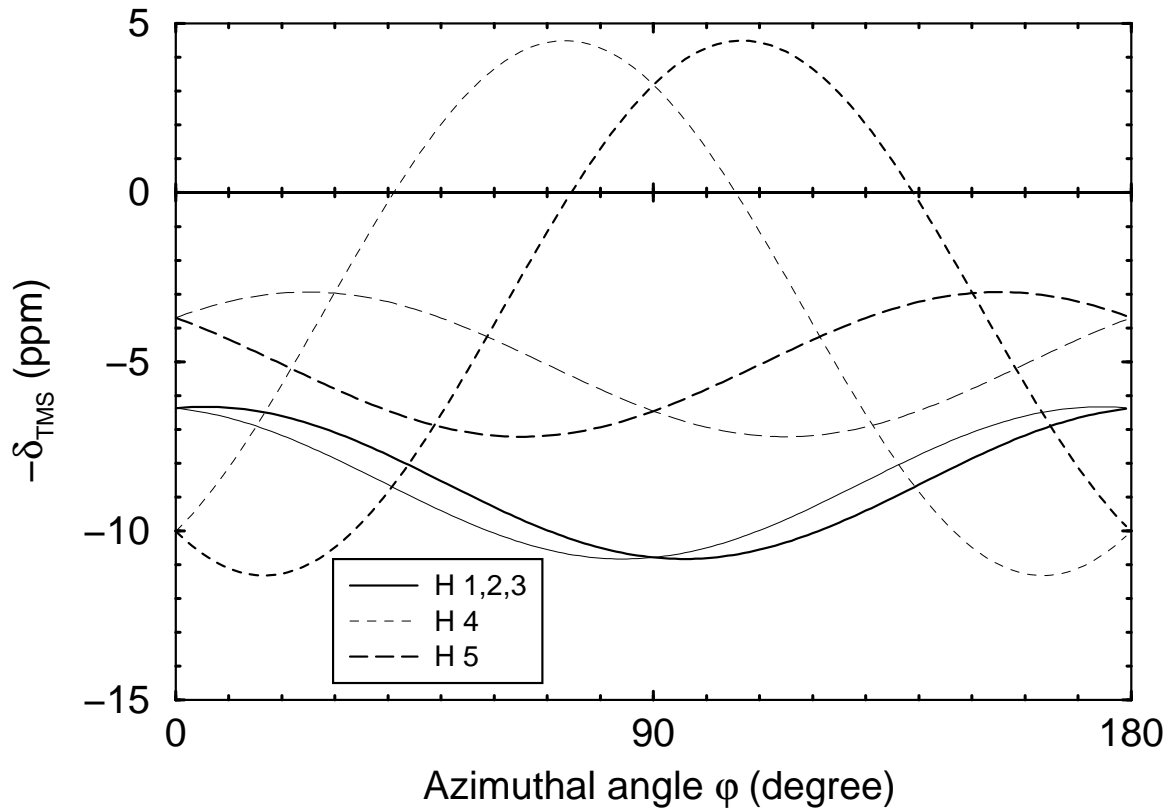
FIG. 3: Angle-dependent chemical shifts of hydrogen along x-axis(a*-axis) calculated from the theoretical chemical shifts tensor. The thick lines represent the first set, and the thin lines represent the second set.
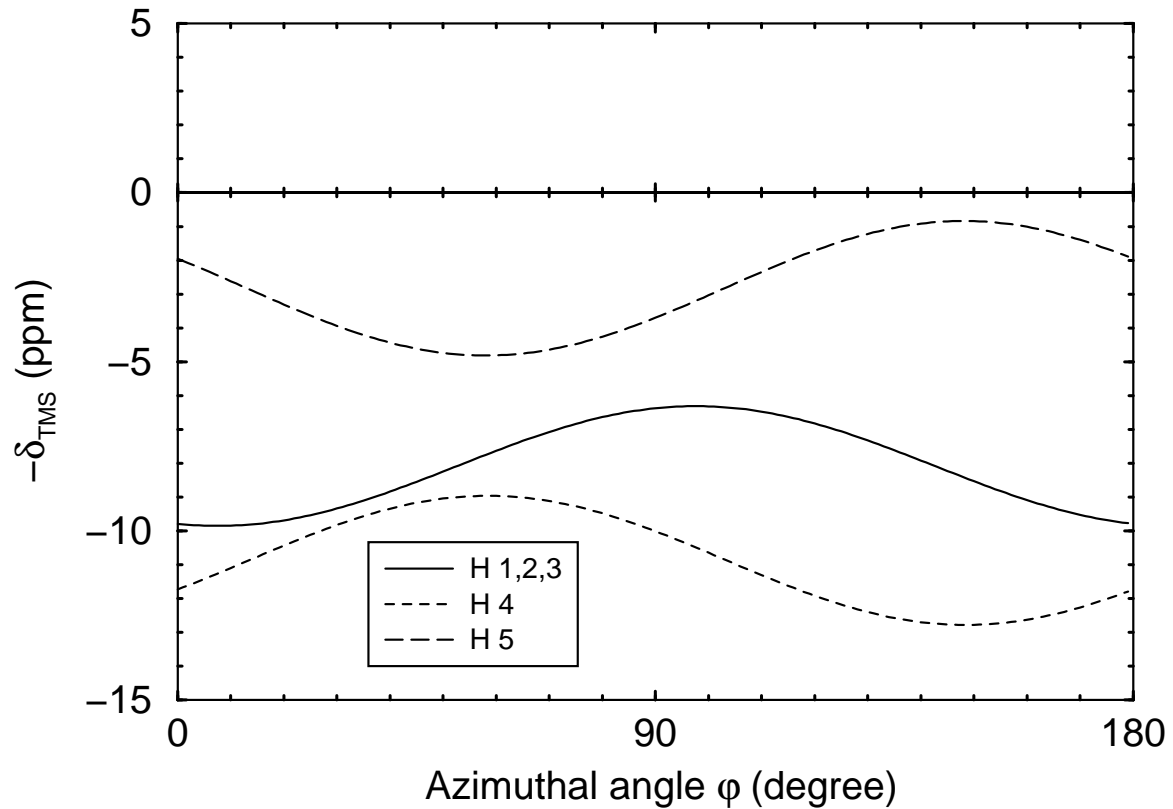
FIG. 4: Angle-dependent chemical shifts of hydrogen along y-axis(b*-axis) calculated from the theoretical chemical shifts tensor. The first set and the second set have the same values.
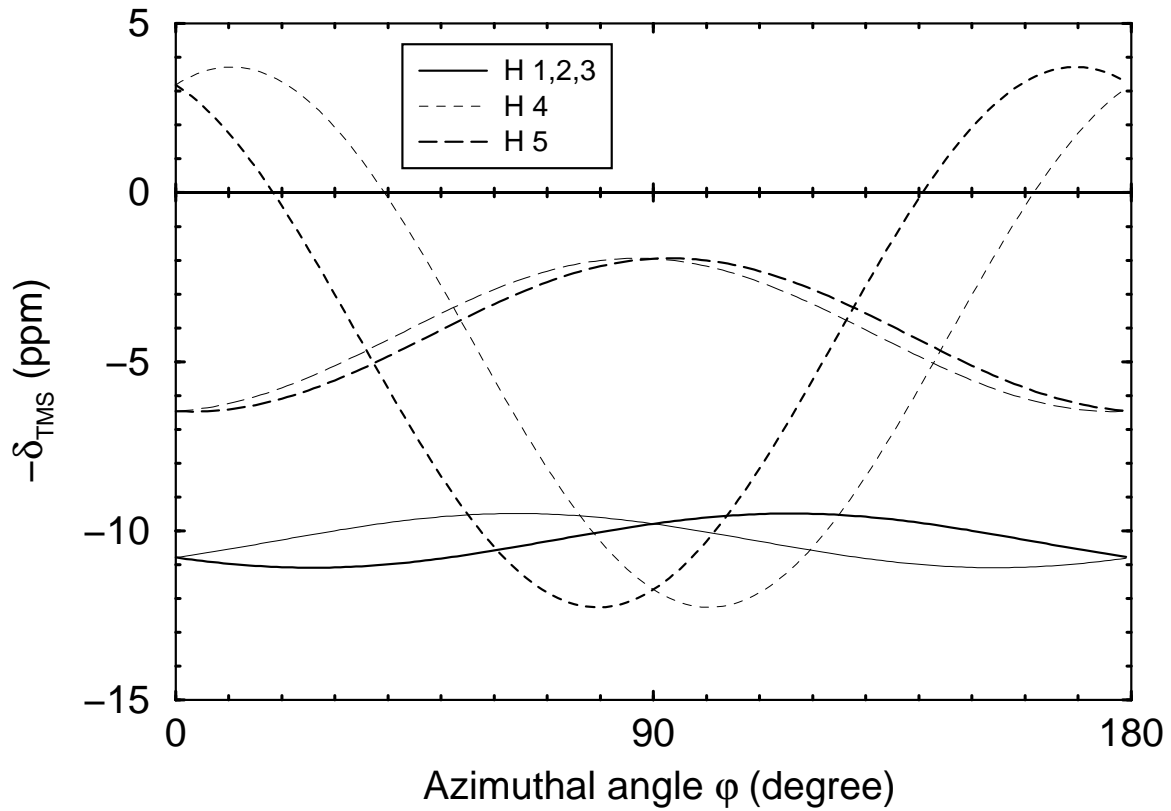
FIG. 5: Angle-dependent chemical shifts of hydrogen along z-axis(c*-axis) calculated from the theoretical chemical shifts tensor. The thick lines represent the first set, and the thin lines represent the second set.
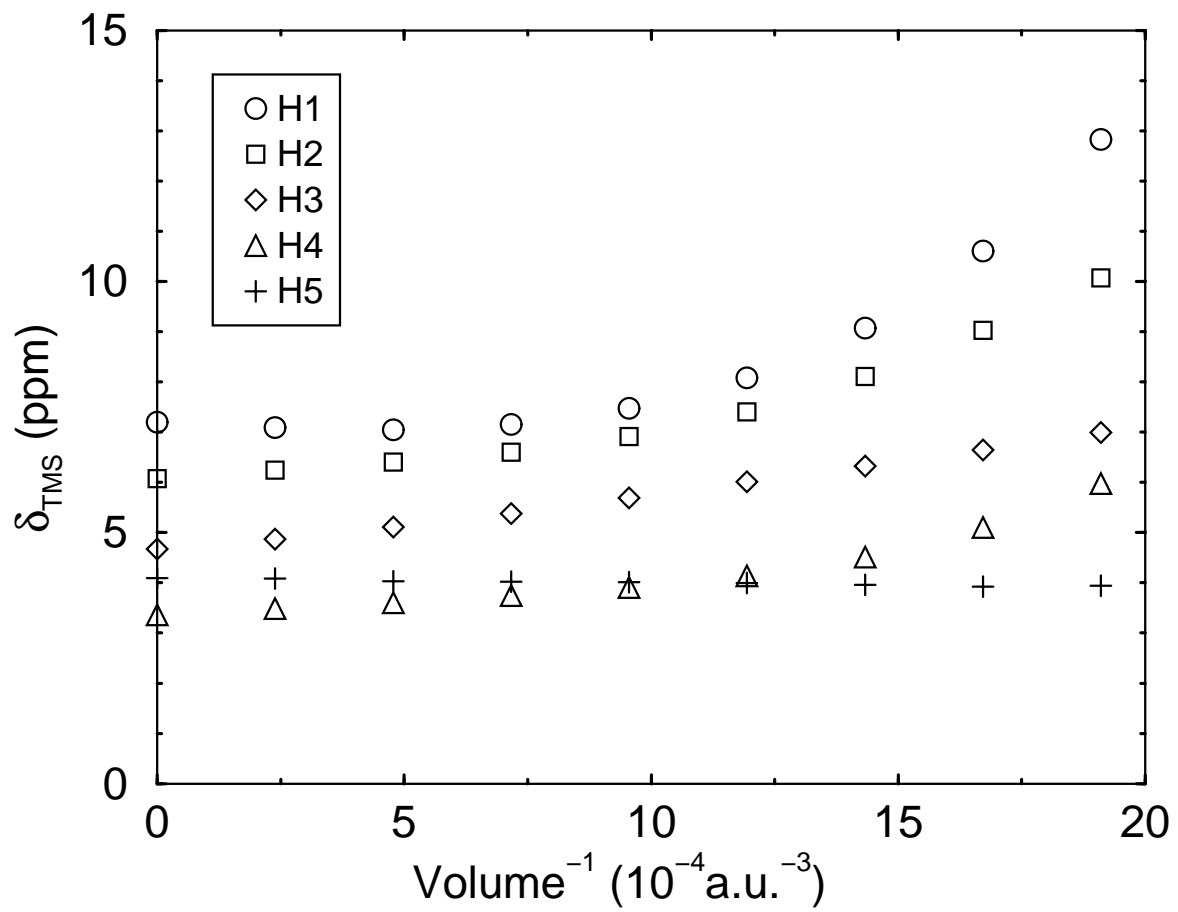
FIG. 6: The effects of environments on the chemical shifts in glycine in intermediate configurations.
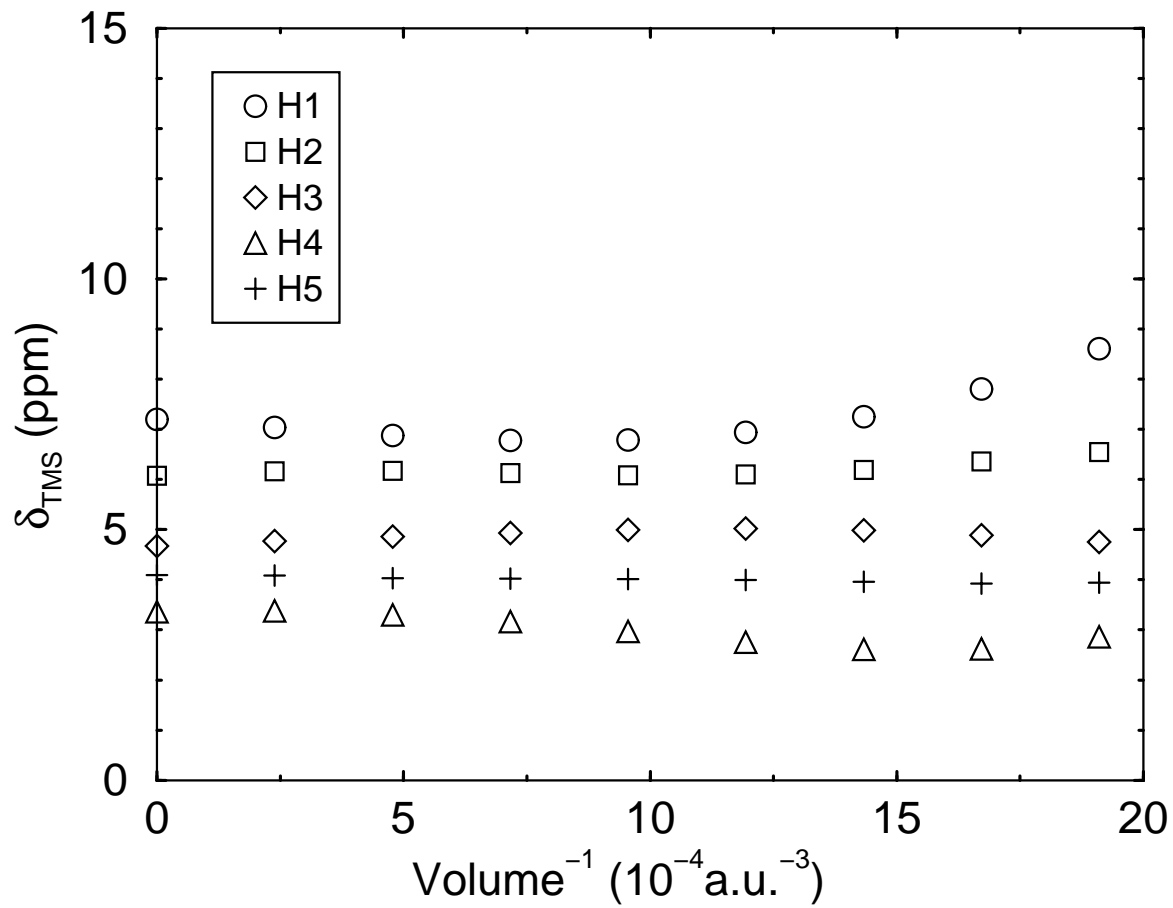
FIG. 7: Proton chemical shifts in glycine after subtracting hydrogen-bonding effects using empirical formula for water, $\delta\sigma[\mathrm{O_{nearest}}] = 138.54$ ppm $\mathrm{au^3/d_{OH}^3}$. H5 has no hydrogen-bond with oxygen atoms, and thus, there is no such subtraction for H5 chemical shifts.